Design of Tunable Flat-top Bandpass Filter Based on Two Long-period Fiber Gratings and Core Mode Blocker

Jinho Bae*

Department of Ocean System Engineering, Jeju National University, Jeju 690-756, Korea

Junkye Bae

Fiber Access 3 Team, LG-Ericsson CO., Ltd. LG R&D Complex, Anyang 431-749, Korea

Sang Bae Lee

Nanophotonics Research Center, KIST, Seoul 130-650, Korea

We propose a tunable flat-top bandpass filter to pass light in a customized wavelength band by using long-period fiber gratings (LPFG) structure. The LPFG structure is composed of a core mode blocker in between two LPFGs. The bandpass spectrum of the proposed structure is obtained in overlapped wavelength band of two LPFGs operating on the same modes. To analyze the properties, we introduce a mathematical matrix model for the structure. We theoretically demonstrate flexibility of the flat-top bandpass filter with various bandwidths.

I. INTRODUCTION

In long-period fiber gratings (LPFG), a fundamental core mode and the multiple cladding modes are coupled, which all propagate in the same (forward) direction. Due to unique features of low insertion loss, low back-reflection and excellent polarization insensitivity, LPFGs have attracted great interest in the optical communications and sensor applications [1, 2]. Some researchers have studied the manufacture of the core mode blocker [3, 4], band pass filter using the core mode blocker [5-7], and tunable bandpass filter using coil heater [8, 9].

The core mode blocker is a device to block off the propagated light in the core, and pass the propagated light in the cladding. Some researchers have developed bandpass filters using LPFGs, and some of them have studied the topics based on a core mode blocker as shown in Fig. 1. In Fig. 1, the LPFG$_1$ is used to interact between core and cladding at resonant wavelength, and light existing in the

core is extinguished by the core mode blocker. The light in the resonant wavelength is propagated through the cladding to the second LPFG. The resonant light existing in the cladding by the LPFG$_2$ is transferred back into the core. The central points of the research are to study the physical phenomenon [3, 4] and the manufacture of the bandpass filter [5-7, 9]. However the design of the flat-top bandpass filter [11] with specific customized wavelength band using an accurate analysis model was not proposed yet.

In the paper, we present the matrix model to analyze the
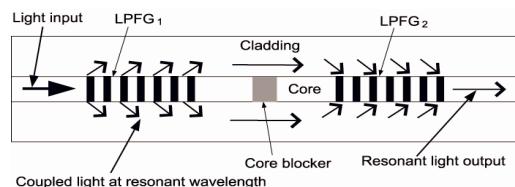
FIG. 1. The LPFG structure with core mode blocker.

---

*Corresponding author: baejh@jejunu.ac.kr

LPFG structures with the core mode blocker. The proposed matrix model is a useful mathematical tool to describe the properties of the structure. We analyze the physical properties of the LPFG structure with a core mode blocker by using the proposed model. By using specially coupled feature of only the same modes in overlapped wavelength region, we demonstrate the design of the flat-top bandpass filter with the customized bandwidth.

II. THE PROPOSED MATHEMATICAL MATRIX MODEL

The structure in Fig. 1 is modeled as the FIR (Finite Impulse Response) filter block diagram as shown in Fig. 2(a). Figure 2(b) is the signal flow graph to analyze both LPFG$_1$ and LPFG$_2$, which is called the multiport lattice filter model [10-12]. Here, D_1 and D_2 are the delay of the diagonal matrix, CB is matrix for core mode blocker, E_{co} and $E_d^{(i)}$ are the E-fields (electric fields) of the fundamental core mode and the ith cladding mode, respectively. And β_{co} and $\beta_{cl}^{(i)}$ are the propagation constant of the fundamental core mode and the ith cladding mode for the LPFGs, L_1 and L_2 are the length of LPFG$_1$ and LPFG$_2$, and d_1, d_2, and d_b are the length for D_1, D_2, and CB.

In Fig. 2(a), the E-fields coming into and out from the structure can be written to be

$$\begin{bmatrix} E_{co}(out) \\ E_{cl}^{(1)}(out) \\ \vdots \\ E_{cl}^{(N)}(out) \end{bmatrix} = Q \begin{bmatrix} E_{co}(in) \\ E_{cl}^{(1)}(in) \\ \vdots \\ E_{cl}^{(N)}(in) \end{bmatrix}, \quad Q \equiv M_2 D_2 C B D_1 M_1 \qquad (1)$$

where $D_k = diag(e^{-j\beta_{co}d_k}, e^{-j\beta_{cl}^{(1)}d_k}, \cdots e^{-j\beta_{cl}^{(N)}d_k})$, $(k = 1, 2)$ are

diagonal matrices and $CB = diag(0, e^{-j\beta_{cl}^{(1)}d_b}, \cdots e^{-j\beta_{cl}^{(N)}d_b})$ is a diagonal matrix with zero determinant.

By assuming the LPFG$_k$, $(k = 1, 2)$ are uniform long period fiber gratings, we can easily get the matrix form of the (N+1)×(N+1) complex matrix M_k, $(k = 1, 2)$ for the LPFG$_k$ with codirectional interactions since the LPFG$_k$ has the multiport lattice filter structure in [10] as follows:

$$M_k \equiv D_G G^{(N)} G^{(N-1)} \cdots G^{(1)}, \qquad (2)$$

where $G^{(p)}$ is (N+1)×(N+1) identity matrix except for the four entries adopted from $F^{(p)}$ in Fig. 2(b). The relation between $G^{(p)}$ and $F^{(p)}$ are as follows:

$$G_{1,1}^{(p)} = F_{1,1}^{(p)}, \quad G_{1,p+1}^{(p)} = F_{1,2}^{(p)}, \quad G_{p+1,1}^{(p)} = -(F_{1,2}^{(p)})^*,$$
$$G_{p+1,p+1}^{(p)} = F_{2,2}^{(p)} = (F_{1,1}^{(p)})^*.$$

(Here, $B_{k,l}$ denotes the (k, l) element of the matrix B.) The matrix D_G represents the phase shift of the LPFG,

$D_G = diag(e^{-j\beta_{co}L_k}, e^{-j\beta_{cl}^{(1)}L_i}, \cdots e^{-j\beta_{cl}^{(N)}L_k})$ and

$$F^{(p)} \equiv \begin{bmatrix} (\cos(S_p L_k) - j\frac{\delta_p}{S_p}\sin(S_p L_k))e^{j\delta_p L_k} & -j\frac{\kappa_p}{S_p}\sin(S_p L_k))e^{j\delta_p L_k} \\ -j\frac{\kappa_p}{S_p}\sin(S_p L_k))e^{-j\delta_p L_k} & (\cos(S_p L_k) + j\frac{\delta_p}{S_p}\sin(S_p L_k))e^{-j\delta_p L_k} \end{bmatrix}, \quad (3)$$

and $S_p \equiv \sqrt{(K_p)^2 + (\delta_p)^2}$, L_k is the length of the LPFG$_k$, δ_p is the detuning factor for the pth cladding mode, and κ_p is the coupling coefficient between the fundamental core mode and the pth cladding mode [10-13].

Note that M_k in (2) can be regarded as a multiport lattice section. Because of the decoupling property of modes, the matrices $G^{(p)}$ in M_k commute with each other so that the


(a)

(b)

FIG. 2. (a) An equivalent block diagram for Fig. 1. (b) Multiport lattice filter model.

2×2 subsections may be interchanged freely. If LPFG$_1$ and LPFG$_2$ are extended as piecewise uniform LPFGs, we can also easily get the M_k using the multiport lattice filter model [10]. Now, the overall transmission coefficient $t \equiv E_{co}(out)/E_{co}(in)$ with $E_{cl}^{(i)}(in) = 0$, $(1 \leq i \leq N)$ is easily seen to be $t = Q_{l,l}$, which is the (1,1)-element of Q.

As shown in Fig. 2(a), after the coupled light on the LPFG$_1$ is absorbed at CB, and then in the LPFG$_2$, the propagated light in the cladding is coupled with the same modes from cladding to core, due to the orthogonality of modes as shown in Fig. 2(b) [10]. Because the overall transmission is calculated as the complex multiplying of two bandpass filters, we cannot get the spectrum in the core if two filters have entirely different bandpass regions.

III. EXAMPLES

We analytically calculated the transmission spectrum curves for the concatenated LPFGs with a core mode blocker in the following examples by computing the transmission coefficient $t = Q_{l,l}$ in (1). The parameters of the fiber used in these examples are as follows:

$n_{co} = 1.449$, $n_{cl} = 1.444$, $n_{ai} = 1$, $r_{co} = 4.5 \mu m$, $r_{cl} = 62.5 \mu m$ where n_{cl} is the refractive index of the cladding, n_{air} is the refractive index of air, r_{co} is the radius of the core, and r_{cl} is the radius of the cladding.
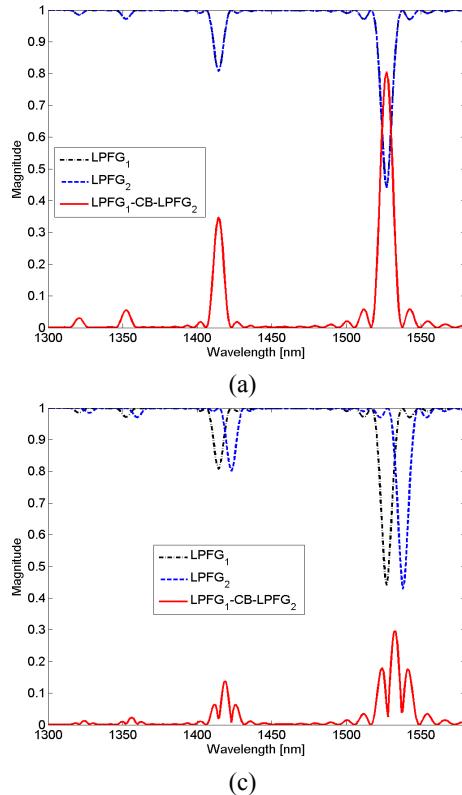
3.1. Example 1 for Uniform LPFG with Both Core Mode Blocker and Delay

Figure 3 shows the transmission for the modes LP_{0i}, ($i = 1, \cdots, 4$) in the wavelength range between 1300 nm and 1580 nm, where LPFG$_1$ and LPFG$_2$ have uniform gratings. Their lengths are $L_1 = 100\Lambda_1$ and $L_2 = 100\Lambda_2$, respectively, the grating period for LPFG$_1$ is $\Lambda_1 = 441.24$ μm, Λ_2 for LPFG$_2$ is varied (441.24 μm for Fig. 3(a), 443.44 μm for Fig. 3(b), 445.65 μm for Fig. 3(c), and 501.28 μm for Fig. 3(d)) and their induced index changes are $\Delta n_1 = n_2 = 0.00011$, respectively. The length of the D$_1$ and the D$_2$ are $d_1 = 400 \Lambda_1$ and $d_2 = 400\Lambda_1$, respectively. The length of the CB is assumed to be $d_b = 0$.

To analyze the properties of the concatenated LPFGs with the core mode blocker, we have calculated the transmission spectra along the change of the Λ_2 as shown in Fig 3. Figures 3(a)-3(c) show the transmission along the overlapped region of the spectrum band of the same modes. We can only get the bandpass spectra by coupling the same modes in the overlapped region. Figure 3(d) shows the transmission for the coupling with the different modes (LP_{04} of LPFG$_1$ and LP_{03} for LPFG$_2$). From the result, we know that the bandpass filter cannot be obtained from coupling the different modes.

3.2. Example 2 for Flat-top Bandpass Filters

We can design a flat-top bandpass filter with the customized bandwidth using the property of coupling with the same modes and the overlapped band. We have synthesized


(a)

(b)

(c)

(d)
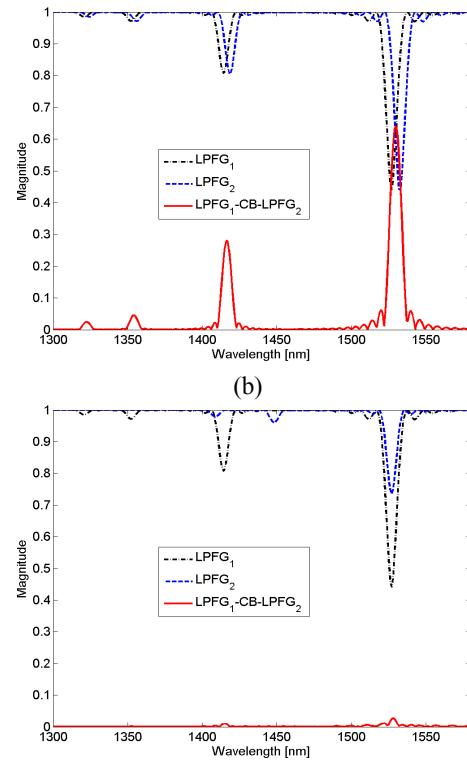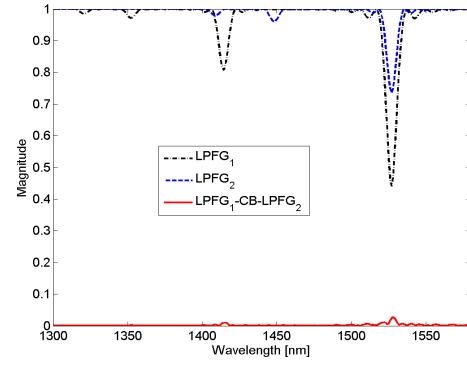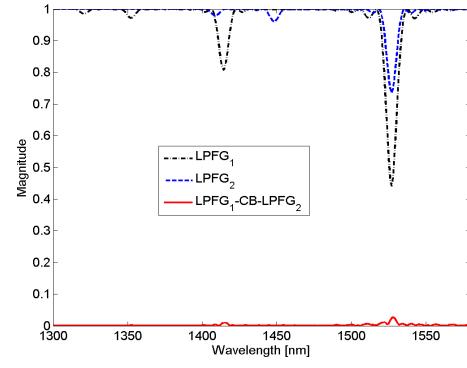
FIG. 3. $\Lambda_1 = 441.24$ μm is fixed and Λ_2 is changed ((a) $\Lambda_2 = 441.24$ μm, (b) $\Lambda_2 = 443.44$ μm (c) $\Lambda_2 = 445.65 \mu m$ and (d) $\Lambda_2 = 501.28$ μm).
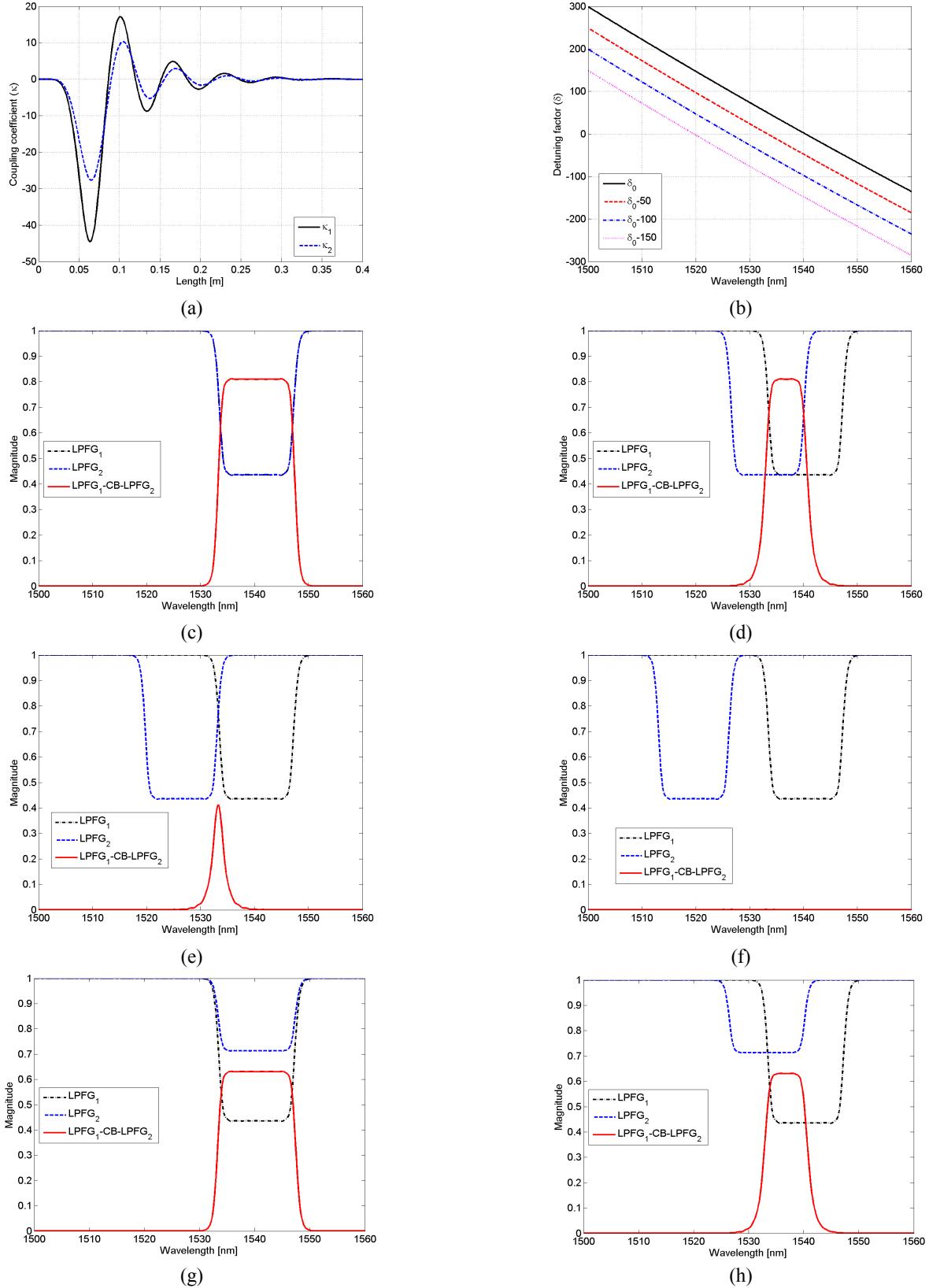
FIG. 4. (a) Coupling coefficients. (b) Detuning factors. (c) The κ_1 and the δ_0 are utilized for the $LPFG_1$ and the $LPFG_2$. (d) $LPFG_1$ (κ_1 and δ_0 is used.) and $LPFG_2$ (κ_1 and δ_0-50 is used.). (e) $LPFG_1$ (κ_1 and δ_0 is used.) and $LPFG_2$ (κ_1 and δ_0-100 is used.). (f) $LPFG_1$ (κ_1 and δ_0 is used.) and $LPFG_2$ (κ_1 and δ_0-150 is used.). (g) $LPFG_1$ (κ_1 and δ_0 is used.) and $LPFG_2$ (κ_2 and δ_0 is used.). (h) $LPFG_1$ (κ_1 and δ_0 is used.) tand $LPFG_2$ (κ_2 and δ_0-50 is used.).

the tunable flat-top filter by considering a single cladding mode as shown in Fig. 4. We have utilized the coupling coefficients κ and the detuning factors δ, respectively, as shown in the Figs. 4(a) and 4(b). The coupling coefficients in Fig. 4(a) can be found by the Gel'fand-Levitan-Marchenko coupled equations [14, 15].

The κ_1 in Fig. 4(a) is used for the $LPFG_1$ and $LPFG_2$ of Figs. 4(c)-4(f). In Fig. 4(b), the δ_0 is used for the $LPFG_1$ and $LPFG_2$ is used the δ_0 for Fig. 4(c), the δ_0-50 for Fig. 4(d), the δ_0-100 for Fig. 4(e), and the δ_0-150 for Fig. 4(f). We have assumed the delay is $d_1 = d_2 = 0$ and the core mode blocker is $CB = diag(0,1,1\cdots,1)$, ideally. The 3dB bandwidth of the $LPFG_1$ and $LPFG_2$ is 13.9 nm. In the case, we can control the bandwidth of the flat-top bandpass filter in the wavelength range less than 13.9 nm $\pm\varepsilon$ (where ε is a small variation by calculating the equation (1).). The 3dB bandwidth of the obtained flat-top filter in Figs. 4(c) and 4(d) are 14.2 nm ($\varepsilon = 0.3$ nm) and 8 nm, respectively.

From the results, we can observe that the bandwidth of the bandpass is changed along the overlapped band region of the flat-top band-rejection of both $LPFG_1$ and $LPFG_2$. If we can make the ideal band-rejection filter, we can synthesize a sharp bandpass filter with the customized bandwidth as well as the bandpass filters with a tunable bandwidth. Especially, if the bandwidth of $LPFG_1$ and $LPFG_2$ aren't overlapped as shown in Fig. 4(f), we cannot synthesize the desired filter.

We also demonstrated the transmission along the overlapped region, when the coupling coefficients are different as shown in Figs. 4(g) and 4(h). The coupling coefficients κ_1 for the $LPFG_1$ and κ_2 the $LPFG_2$ are utilized as shown in Fig. 4(a). The detuning factors δ for Figs. 4(g) and 4(h) are the same ones as for Figs. 4(c) and 4(d). We have also used the delay and the core mode blocker as above examples.

From the Figs 4(g) and 4(h), we have obtained similar results to Figs. 4(c) and 4(d) although the $LPFG_1$ and $LPFG_2$ have different magnitude levels. The 3 dB bandwidth of the $LPFG_2$ is 14.1 nm. The 3 dB bandwidth of the obtained flat-top filter in Figs. 4(c) and 4(d) are 14.2 nm($\varepsilon = 0.1$ nm) and 8 nm, respectively. The results show that the magnitude level of the flat-top bandpass filter is dependent on the magnitudes of the $LPFG_1$ and $LPFG_2$.

IV. CONCLUSION

The analytical model for the LPFG with the core mode blocker is proposed. We have also analyzed and described the physical phenomenon of the structure by using the proposed model. We have proposed a design method of the flat-top bandpass filter with customized bandwidth. We have also demonstrated, through computer simulations, the bandwidth of the flat-top filters controlled by tuning the overlapped band region.

REFERENCES

1. A. Othonos and K. Kalli, *Fiber Bragg Gratings - Fundamentals and Applications in Telecommunications and Sensing* (Artech House, Boston, USA, 1999).
2. S. Kim, G. H. Kim, K. Hwang, S. D. Lim, K. Lee, S. H. Kim, S. B. Lee, and J. Jeong, "Investigation of an arc-induced long period fiber grating inscribed in a photonic crystal fiber with two large air holes," J. Opt. Soc. Korea **13**, 428-433 (2009).
3. Y. G. Han, S. H. Kim, S. B. Lee, U. C. Paek, and Y. Chung, "Development of core mode blocker with H_2-loaded Ge-B codoped fibres," Electron. Lett. **39**, 1107-1108 (2003).
4. S. D. Lim, J. G. Kim, K. Lee, S. B. Lee, and B. Y. Kim, "Fabrication of a highly efficient core-mode blocker using a femtosecond laser ablation technique," Opt. Express **17**, 18449-18454 (2009).
5. S. Choi, T. J. Eom, J. W. Yu, B. H. Lee, and K. Oh, "Novel all-fiber bandpass filter based on hollow optical fiber," IEEE Photon. Technol. Lett. **14**, 1701-1703 (2002).
6. S. Choi, T. J. Eom, J. W. Yu, and B. H. Lee, "Broad-band tunable all-fiber bandpass filter based on hollow optical fiber and long-period grating pair," IEEE Photon. Technol. Lett. **17**, 115-117 (2005).
7. H. Sakata, Y. Takata, and S. Suzuki, "Single-channel bandpass filter based on vernier-aligned long-period fiber gratings," IEEE Photon. Technol. Lett. **19**, 1661-1663 (2007).
8. D. S. Starodubov, V. Grubsky, and J. Feinberg, "All-fiber bandpass filter with adjustable transmission using cladding-mode coupling," IEEE Photon. Technol. Lett. **10**, 1590-1592 (1998).
9. Y. Han, S. H. Kim, and S. B. Lee, "Flexibly tunable multi-channel filter and bandpass filter based on long-period fiber gratings," Opt. Express **12**, 1902-1907 (2004).
10. J. Bae, J. Chun, and S. B. Lee, "Synthesis of long-period fiber gratings with the inverted erbium gain spectrum using the multiport lattice filter model," J. Ligthwave Technol. **22**, 1976-1986 (2004).
11. H. Kim, J. Bae, and J. Chun, "Synthesis of flat-top bandpass filters using two-band rejection long-period fiber gratings," IEEE Photon. Technol. Lett. **19**, 1466-1468 (2007).
12. H. Kim, J. Bae, J. W. Lee, J. Chun, and S. B. Lee, "Analysis of concatenated longperiod fiber gratings having phase-shifted and cascaded effects," Jpn. J. Appl. Phys. Part 1 **42**, 5098-5101 (2003).
13. M. Yi, Y. Kim, D. Yee, and J. Ahn, "Terahertz frequency spreading filter via one-dimensional dielectric multilayer structures," J. Opt. Soc. Korea **13**, 398-402 (2009).
14. G. Song and S. Shin, "Design of corrugated waveguide filters by the Gel'fand-Levitan-Marchenko inverse-scattering method," J. Opt. Soc. Am. A **2**, 1905-1915 (1985).
15. E. Peral, J. Capmany, and J. Marti, "Iterative solution to the Gel'fand-Levitan-Marchenko coupled equations and application to synthesis of fiber gratings," J. Quantum Electron. **32**, 2078-2084 (1996).